

Effects of Hall Current on MHD Free and Forced Convection flow of Newtonian fluid through a Porous medium in an Infinite vertical plate in presence of Thermal radiation heat transfer and surface temperature oscillation

¹E.Neeraja and ²M.Veera Krishna

¹Department of Mathematics, M.S.Thakur college of sciences, Seawoods, Nerul, Navi Mumbai (Maharashtra) - 400706 (INDIA)

²Department of Mathematics, Rayalaseema University, KURNOOL (A.P) - 518002 (INDIA)

ABSTRACT

In this paper, we study the steady and unsteady magneto hydro dynamic (MHD) viscous, incompressible free and forced convective flow of an electrically conducting Newtonian fluid through a porous medium in the presence of appreciable thermal radiation heat transfer and surface temperature oscillation taking hall current into account. The fluid is assumed to be optically-thin and magnetic Reynolds number small enough to neglect induced hydro magnetic effects. Secondary (cross-flow) effects are incorporated. The governing equations are solved analytically using complex variables. Detailed computations of the influence of governing parameters on the unsteady mean flow velocity (u_1) and unsteady mean cross flow velocity (w_1), the plate shear stresses for the unsteady main and the secondary flow and also temperature gradients due to the unsteady main flow and the unsteady cross flow, are presented graphically and tabulated. The closed-form solutions reveal that the shear stress component due to a steady mean flow experiences a non-periodic oscillation which varies as a function of the Hartmann number (M^2) and radiation parameter (K_1). However the shear stress components due to main and cross flows for an unsteady mean flow are subjected to periodic oscillation which depends on Hartmann number, inverse Darcy parameter, radiation parameter but also on the Prandtl number and frequency of oscillation. Applications of the model include fundamental magneto-fluid dynamics, MHD energy systems and magneto-metallurgical processing for aircraft materials.

Keywords: steady and unsteady flows, thermal radiation heat transfer, hall current effects, free and forced convective flows, surface temperature oscillation and porous medium.

Keywords - About five key words in alphabetical order, separated by comma

I. INTRODUCTION

Several authors have considered thermal radiation effects on convection flows with and without magnetic fields. A seminal study was communicated by Audunson and Gebhart [5] who also presented rare experimental data for radiation-convection boundary layer flows of air, argon and ammonia, showing that thermal radiation increases convective heat transfer by up to 40 %. Larson and Viskanta [15] investigated experimentally the unsteady natural convection-radiation in a rectangular enclosure for the case of fire-generated thermal radiative flux, showing that thermal radiation dominates the heat transfer in the enclosure and alters the convective flow patterns substantially. Helliwell and Mosa [12] reported on thermal radiation effects in buoyancy-driven hydro magnetic flow in a horizontal channel flow with an axial temperature gradient in the presence of Joule and viscous heating. Bestman [6] studied magneto hydro dynamic rarefied oscillatory heat transfer from a plate with significant thermal radiation using a general differential approximation for radiation flux and perturbation methods for small amplitude oscillations. Yasar and Moses [23] developed a one-dimensional adaptive-grid finite-differencing computer code for thermal radiation magneto hydro dynamic (RMHD) simulations of fusion plasmas. Alagoa *et al.* [2] studied magneto hydro dynamic optically-transparent free-convection flow, with radiative heat transfer in porous media with time-dependent suction using an asymptotic approximation, showing that thermal radiation exerts a significant effect on the flow dynamics. El-Hakim [10] analyzed thermal radiation effects on transient, two dimensional hydro magnetic free convection along a vertical surface in a highly porous medium using the Rosseland diffusion approximation for the radiative heat flux in the energy equation, for the case where free-stream velocity of the fluid vibrates about a mean constant value and the surface absorbs the fluid with constant velocity. Israel-Cookey *et al.* [14] described the effects of viscous dissipation and thermal radiation on transient magneto hydro dynamic free-

convection flow past an infinite vertical heated plate in an optically thin environment with time-dependent suction showing that increased cooling (positive Grashof number) of the plate and increasing Eckert number boost velocity profile and temperature, a rise in magnetic field, thermal radiation and Darcian drag force decelerate the flow and increasing thermal radiation and magnetic field cool the flow in the porous medium. Other excellent studies of thermal radiation-convection magneto hydro dynamics include Duwairi and Damseh [8], Raptis *et al.* [18] who considered axi-symmetric flow and Duwairi and Duwairi [9] who studied thermal radiation heat transfer effects on the hydro magnetic Rayleigh flow of a gray viscous fluid. Vasil'ev and Nesterov [22] who presented a two dimensional numerical model for radiative-convective heat transfer in the channel of an MHD generator with a self-sustaining current layer. Duwairi [7] considered Ohmic and viscous dissipation effects on thermal radiating hydro magnetic convection. Ouaf [17] has considered thermal radiation effects on hydro magnetic stretching porous sheet flow. Aboeldahab and Azzam [1] have described the effects of magnetic field on hydro magnetic mixed free-forced heat and mass convection of a gray, optically-thick, electrically-conducting viscous fluid along a semi-infinite inclined plate for high temperature and concentration using the Rosseland approximation. Zueco [24] has modeled using the network simulation technique, the collective effects of wall transpiration, thermal radiation and viscous heating effects on hydro magnetic unsteady free convection flow over a semi-infinite vertical porous plate for a non-gray fluid (absorption coefficient dependent on wave length). Alam *et al.* [3] have very recently investigated the influence of thermal radiation, variable suction and thermo phoretic particle deposition on steady hydro magnetic free-forced convective heat and mass transfer flow over an infinite permeable inclined plate using the Nachtsheim-Swigert shooting iteration technique and a sixth-order Runge-Kutta integration scheme. Ghosh and Pop [11] have studied thermal radiation of an optically-thick gray gas in the presence of indirect natural convection showing that the pressure rise region leads to increase in the velocity with an increase of radiation parameter. Recently Anwerbeg. O and S.K, Ghosh [4] investigated hydro magnetic free and forced convection of an optically-thin gray gas from vertical flat plate subject to a surface temperature oscillation with significant thermal radiation. In this paper, we study the steady and unsteady magneto hydro dynamic (MHD) viscous, incompressible free and forced convective flow of an electrically conducting Newtonian fluid through a porous medium in the presence of appreciable thermal radiation heat transfer and

surface temperature oscillation taking hall current into account.

II. FORMULATION AND SOLUTION OF THE PROBLEM

We consider a two dimensional unsteady MHD flow of a viscous incompressible electrically conducting fluid occupying a semi infinite region of space bounded by porous medium through an infinite vertical plate moving with the constant velocity U , in the presence of a transverse magnetic field. The surface temperature of the plate oscillates with small amplitude about a non-uniform mean temperature. The co-ordinate system is such that the x-axis is taken along the plate and y-axis is normal to the plate. A uniform transverse magnetic field B_0 is imposed parallel to y-direction. All the fluid properties are considered constant except the influence of the density variation in the buoyancy term, according to the classical Boussinesq approximation. The radiation heat flux in the x-direction is considered negligible in comparison to the y-direction. The unsteady MHD equation governing the fluid through a porous medium under the influence of transverse magnetic field with buoyancy force, then takes the vectorial form,

$$\frac{\partial \mathbf{q}}{\partial t} + (\mathbf{q} \cdot \nabla) \mathbf{q} = \nu \nabla^2 \mathbf{q} + \frac{1}{\rho} \mathbf{J} \times \mathbf{B} + g\beta(T - T_\infty) \quad (2.1)$$

The equation of continuity is

$$\nabla \cdot \mathbf{q} = 0 \quad (2.2)$$

Ohm's law for a moving conductor states

$$\mathbf{J} = \sigma(\mathbf{E} + \mathbf{q} \times \mathbf{B}) \quad (2.3)$$

Maxwell's electromagnetic field equations are

$$\nabla \times \mathbf{B} = \mu_e \mathbf{J} \text{ (Ampere's Law)} \quad (2.4)$$

$$\nabla \times \mathbf{E} = -\frac{\partial \mathbf{B}}{\partial t} \text{ (Faraday's Law)} \quad (2.5)$$

$$\nabla \cdot \mathbf{B} = 0 \text{ (Solenoidal relation i.e., magnetic field continuity)} \quad (2.6)$$

$$\nabla \cdot \mathbf{J} = 0 \text{ (Gauss's Law i.e., Conservation of electric charge)} \quad (2.7)$$

In which \mathbf{q} , \mathbf{B} , \mathbf{E} and \mathbf{J} are, respectively, the velocity vector, magnetic field vector, electric field vector and current density vector, T is the temperature of the fluid, T_∞ is the temperature far away the plate, g is the gravitational acceleration, β is the coefficient of volume expansion, ρ is the density of fluid, σ is the electrical conductivity, μ_e is the magnetic permeability of the fluid, t is time, ν is dynamic viscosity and B_0 is the magnetic flux density component normal to the plate surface. According to Shercliff [20] and Hughes and young [13], the following assumptions are compatible with the fundamental equations (2.1) to (2.7) of magneto hydro dynamics.

$$\mathbf{q} = (u, 0, w), \mathbf{B} = (B_x, B_0, B_z) \quad (2.8)$$

$$\mathbf{E} = (E_x, E_y, E_z), \mathbf{J} = (J_x, 0, J_z) \quad (2.9)$$

Where, u and w are the velocity components along the x -direction and z -direction respectively. Since magnetic Reynolds number is very small for metallic liquid or partially ionized fluid the induced magnetic field produced by the electrically conducting fluid is negligible. Also as no external electric field is applied, the polarization voltage is negligible so that following Meyer [16], $E=0$. Ohmic and viscous heating effects are also neglected. The appropriate boundary conditions to be satisfied by equations (2.1) and (2.3) are

$$u' = U, w' = 0, \Phi = T - T_\infty = \theta_w(x)(1 + \zeta e^{i\omega t}), \text{ at } y' = 0; \\ u' \rightarrow 0, w' \rightarrow 0, \Phi \rightarrow 0 \quad \text{at } y' \rightarrow \infty; \quad (2.10)$$

Where Φ designated wall-free stream temperature difference, $\zeta = \frac{U}{v}$ i.e., dimensionless velocity ratio and ω is the frequency of oscillation in the surface temperature of the plate. The conditions (2.10) suggest solutions to equations (2.1) to (2.3) for the variables u', v' and Φ of the form,

$$u' = u'_0 + \varepsilon e^{i\omega t} u'_1, \quad (2.11)$$

$$w' = w'_0 + \varepsilon e^{i\omega t} w'_1, \quad (2.12)$$

$$\Phi = \theta_w(x)(\theta'_0 + \zeta e^{i\omega t} \theta'_1) \quad (2.13)$$

Since $\bar{B} = (0, B_0, 0)$ and $\bar{q} = (u, 0, w)$, When the strength of the magnetic field is very large, the generalized Ohm's law is modified to include the Hall current, so that

$$J + \frac{\omega_e \tau_e}{H_0} J \times H = \sigma (E + \mu_e q \times H) \quad (2.14)$$

Where, q is the velocity vector, H is the magnetic field intensity vector, E is the electric field, J is the current density vector, ω_e is the cyclotron frequency, τ_e is the electron collision time, σ is the fluid conductivity and, μ_e is the magnetic permeability. In the above equation the electron pressure gradient, the ion-slip and thermo-electric effects are neglected. We also assume that the electric field $E=0$ under assumptions reduces to

$$J_x + m J_z = \sigma \mu_e H_0 w \quad (2.15)$$

$$J_z - m J_x = -\sigma \mu_e H_0 u \quad (2.16)$$

On solving these equations (2.15) and (2.16), we have,

$$J_x = \frac{\sigma \mu_e H_0}{1 + m^2} (w + mu), J_y = 0, J_z = \frac{\sigma \mu_e H_0}{1 + m^2} (mw - u)$$

Where $m = \tau_e \omega_e$ is the hall parameter.

For the case of an optically-thin gray gas, the thermal radiation flux gradient may be expressed as follows (Siegel and Howell [21])

$$-\frac{\partial q_r}{\partial y'} = 4a\sigma^*(T_\infty'^4 - T'^4) \quad (2.18)$$

and q_r is the radiative heat flux, a is absorption coefficient of the fluid and σ^* is the Stefan-Boltzmann constant. We assume that the temperature differences within the flow are sufficiently small such that T'^4 may be expressed as a linear function of the temperature. This is accomplished by expanding T'^4 in a Taylor series about T_∞' and neglecting higher order terms, leading to:

$$T'^4 = 4T_\infty'^3 T' - 3T_\infty'^4 \quad (2.19)$$

Making use of the equation (2.17) the components u'_0, w'_0 and θ'_0 represent the steady mean flow and temperature fields, and satisfy the following equations:

$$\frac{\partial u'_0}{\partial x'} + \frac{\partial w'_0}{\partial y'} = 0 \quad (2.20)$$

$$0 = v \frac{\partial^2 u'_0}{\partial y'^2} + g\beta\theta_w(x)\theta'_0 + \frac{\sigma \mu_e H_0}{1 + m^2} (mw'_0 - u'_0) - \frac{v}{k} u'_0 \quad (2.21)$$

$$0 = v \frac{\partial^2 w'_0}{\partial y'^2} - \frac{\sigma \mu_e H_0}{1 + m^2} (w'_0 + mu'_0) - \frac{v}{k} w'_0 \quad (2.22)$$

$$0 = \frac{K}{\rho c_p} \frac{\partial^2 \theta'_0}{\partial y'^2} - \frac{1}{\rho c_p} \frac{\partial q_r}{\partial y'} \quad (2.23)$$

Where K designates thermal conductivity and c_p is the specific heat capacity under constant pressure. The corresponding boundary conditions are

$$u'_0 = U, w'_0 = 0, T = T_w \quad \text{at } y' = 0 \quad (2.24)$$

$$u'_0 = 0, w'_0 \rightarrow 0, T \rightarrow T_\infty \quad \text{at } y' \rightarrow \infty \quad (2.25)$$

Again making use of the equation (3.17), the components u'_1, w'_1 and θ'_1 represent the steady mean flow and temperature fields, and satisfying the following equations:

$$\frac{\partial u'_1}{\partial x'} + \frac{\partial w'_1}{\partial y'} = 0 \quad (2.26)$$

$$i\omega u'_1 = v \frac{\partial^2 u'_1}{\partial y'^2} + g\beta\theta_w(x)\theta'_1 + \frac{\sigma \mu_e H_0}{1 + m^2} (mw'_1 - u'_1) - \frac{v}{k} u'_1 \quad (2.27)$$

$$i\omega w'_1 = v \frac{\partial^2 w'_1}{\partial y'^2} - \frac{\sigma \mu_e H_0}{1 + m^2} (w'_1 + mu'_1) - \frac{v}{k} w'_1 \quad (2.28)$$

$$\frac{\partial \Phi}{\partial t} = \frac{K}{\rho c_p} \frac{\partial^2 \theta'_1}{\partial y'^2} - \frac{1}{\rho c_p} \frac{\partial q_r}{\partial y'} \quad (2.29)$$

The corresponding boundary conditions are

$$u'_1 = U, w'_1 = 0, T = T_w \quad \text{at } y' = 0 \quad (2.30)$$

$$u'_1 \rightarrow 0, w'_1 \rightarrow 0, T \rightarrow T_\infty \quad \text{at } y' \rightarrow \infty \quad (2.31)$$

Proceeding with the analysis we introduce dimensionless quantities to normalize the flow model:

$$u_0 = \frac{u'_0}{U}, w_0 = \frac{w'_0}{U}, u_1 = \frac{u'_1}{U}, w_1 = \frac{w'_1}{U}, y = \frac{y'U}{\nu}$$

$$t = \frac{t'U^2}{\nu}, \theta_0 = \frac{\theta_0 y}{UL}, \theta_1 = \frac{\theta_1 y}{ULe}, Gr = \frac{g\beta\nu^2\theta_w(x)}{U^4L}$$

$$\omega = \frac{\omega'\nu}{U^2}, M^2 = \frac{\sigma B_0^2\nu}{\rho U^2}, D^{-1} = \frac{\wp^2}{k\nu^2}, K_1 = \frac{16a\sigma\nu^2 T_\infty^3}{KU^2}$$

$$\theta_0 = \theta_1 = \frac{T - T_\infty}{T_w - T_\infty}$$

Where Gr is Grashof number, M^2 is the Hartmann (magneto hydro dynamic number), K_1 is the thermal radiation-conduction number, K is thermal conductivity and θ_1 is dimensionless temperature D^{-1} is the inverse Darcy parameter. Using equation (2.29) together with the equations (2.18) and (2.19) the dimensionless form of equation (2.23) becomes:

$$\frac{d^2\theta_0}{dy^2} - K_1\theta_0 = 0 \quad (2.32)$$

Making use of non-dimensional variables, together with equations (2.18) and (2.19) the dimensionless form of equation (2.29) becomes:

$$\frac{d^2\theta_1}{dy^2} - (K_1 + i\omega Pr)\theta_1 = 0 \quad (2.33)$$

We are introducing complex variables

$$u_0 + iw_0 = F, \quad (2.34)$$

$$u_1 + iw_1 = H \quad (2.35)$$

where $i = \sqrt{-1}$.

Combining equations (2.21) and (2.22) with the help of (2.34), the differential equation for steady mean flow in dimensionless form becomes:

$$\frac{d^2F}{dy^2} - \left(\frac{M^2}{1+m^2} + D^{-1}\right)F = -Gr\theta_0 \quad (2.36)$$

Combining equations (2.27) and (2.28) with the help of (2.35), the differential equation for unsteady mean flow in dimensionless form reduces to:

$$\frac{\partial^2 H}{\partial y^2} - \left(\frac{M^2}{1+m^2} + D^{-1} + i\omega\right)H = -Gr\theta_1 \quad (2.37)$$

The corresponding boundary conditions for steady mean flow (non-dimensional) are

$$u_0 = 1, w_0 = 0, \theta_0 = 1 \text{ at } y = 0 \quad (2.38)$$

$$u_0 = 0, w_0 = 0, \theta_0 = 0 \text{ at } y \rightarrow \infty \quad (2.39)$$

The corresponding boundary conditions for unsteady mean flow (non-dimensional) are

$$u_1 = 1, w_1 = 0, \theta_1 = 1 \text{ at } y = 0 \quad (2.40)$$

$$u_1 = 0, w_1 = 0, \theta_1 = 0 \text{ at } y \rightarrow \infty \quad (2.41)$$

The boundary conditions (2.38), (2.39), (2.40) and (2.41) can be written subject to equation (2.34 and 2.35) as follows:

$$F = 1, \theta_0 = 1 \text{ at } y = 0 \quad (2.42)$$

$$F = 0, \theta_0 = 0 \text{ at } y \rightarrow \infty \quad (2.43)$$

and

$$H = 1, \theta_1 = 1 \text{ at } y = 0 \quad (2.44)$$

$$H = 0, \theta_1 = 0 \text{ at } y \rightarrow \infty \quad (2.45)$$

Equations (2.36) and (2.32) subjects to the boundary conditions (2.42) and (2.43) can be solved and the solution for the steady mean flow can be expressed as:

$$F = u_0(y) + iw_0(y) = e^{-\left(\frac{M^2}{1+m^2} + D^{-1}\right)y} + \frac{Gr}{K_1 - \left(\frac{M^2}{1+m^2} + D^{-1}\right)} \left[e^{\left(\frac{M^2}{1+m^2} + D^{-1}\right)y} - e^{-\sqrt{K_1}y} \right] \quad (2.46)$$

in which $-e^{-\sqrt{K_1}y} = \theta_0(y)$.

Equations (2.36) and (2.33) subjects to the boundary conditions (2.44) and (2.45) may also be solved yielding the following solution for unsteady mean flow:

$$H = u_1(y,t) + iw_1(y,t) = e^{-(C_1+iD_1)y} + \frac{\alpha - i\beta}{\alpha^2 + \beta^2} Gr \left[e^{-(C_1+iD_1)y} - e^{-(C_2+iD_2)y} \right] \quad (2.47)$$

and $\theta_1(y,t) = e^{-\sqrt{K_1+i\omega Pr}y}$.

Where, the functions θ_0 and θ_1 denote the temperature fields due to the main flow and cross flows, respectively. Of interest in practical MHD plasma energy generator design are the dimensionless shear stresses at the plate, which may be defined for steady and unsteady mean flow, respectively as follows:

$$\frac{dF}{dy}\Big|_{y=0} = -\left(\sqrt{\frac{M^2}{1+m^2} + D^{-1}}\right) + \frac{Gr}{K_1 - \left(\frac{M^2}{1+m^2} + D^{-1}\right)} \left[-\left(\sqrt{\frac{M^2}{1+m^2} + D^{-1}}\right) + \sqrt{K_1} \right] \quad (2.48)$$

$$\frac{\partial H}{\partial y}\Big|_{y=0} = -(C_1 + iD_1) + \frac{\alpha - i\beta}{\alpha^2 + \beta^2} Gr \left[-(C_1 + iD_1) + (C_2 + iD_2) \right] \quad (2.49)$$

It is evident from equations (2.48) and (2.49) that the shear stress component due to the main flow for the steady mean flow equations (2.48) and the shear stress components due to main and cross flows given by equation (2.49) do not vanish at the plate. Inspection of these expressions also reveals that the shear stress component as defined by equation (2.48) due to a steady mean flow is subjected to a non-periodic oscillation that depends on Hartmann number, inverse Darcy parameter and radiation- conduction parameter. In contrast to this,

the shear stress components as computed in equation (2.49) due to the main and cross flows for an unsteady mean flow are subjected to periodic oscillation which is a function of not only Hartmann number and radiation- conduction parameter, but also the Prandtl number and the frequency of oscillation. The shear stress for equation (2.48) will vanish at the plate ($y=0$) at a critical value of the free convection parameter i.e. Grashof number, defined by the condition:

$$Gr_{crit} = \sqrt{\frac{M^2}{1+m^2} + D^{-1}} \left(\sqrt{K_1} + \sqrt{\frac{M^2}{1+m^2} + D^{-1}} \right) \quad (2.50)$$

The shear stress for equation (2.48) will vanish at the plate ($y=0$) when

$$Gr_{crit} = (C_1 + iD_1)[(C_1 + C_2) + i(D_1 + D_2)] \quad (2.51)$$

Also of interest in plasma MHD generator design is the dimensionless temperature gradient at the plate. This can be shown to take the form, for the unsteady main flow, as follows:

$$\frac{d\theta_0}{dy} \Big|_{y=0} = -\sqrt{K_1} \quad (2.52)$$

For the unsteady cross flow the dimensionless temperature gradient at the plate ($y=0$) is

$$\frac{d\theta_1}{dy} \Big|_{y=0} = -\sqrt{K_1 + i\omega Pr} \quad (2.53)$$

Comparing equations (2.51) and (2.52) it is immediately deduced that in the absence of an oscillating surface i.e., for $\omega=0$, the dimensionless temperature gradient due to a steady and unsteady mean follows are identical.

III. RESULTS AND DISCUSSION

The flow governed by the non-dimensional parameters namely viz., Hartmann number M , inverse Darcy parameter D^{-1} , hall parameter m , K_1 is the thermal radiation-conduction number, surface temperature oscillation i.e., ω and Grashof number Gr . Selected computations for the velocity and temperature fields have been provided in figures (1-17) & (18-24) respectively. Default values of the dimensionless thermo-physical parameters were specified as follows, unless otherwise indicated: $M = 2$, $m=1$, $K_1 = 1$, $\omega = 2$, $Gr = 2$ and $Pr = 0.025$ which correspond to weak free convection currents in liquid metal flow under strong magnetic field with equal thermal radiation and thermal conduction contribution, with surface temperature oscillation. Computations for the shear stresses at the plate are provided in tables (1-3) and for temperature gradient at the plate in tables (4-7).

We note that steady mean flow is simulated for which there will be no surface temperature oscillation i.e. $\omega = 0$. The magnitude of the velocity reduces with increase in the intensity of the magnetic field. i.e., Mean flow velocity, (u_0) is

continuously reduced with increasing M . The transverse magnetic field generates a retarding body force in the opposite direction to the flow which serves to decelerate the flow. As such magnetic field is an effective regulatory mechanism for the regime (Fig. 1). The magnitude of the velocity (u_0) reduces with increase in the inverse Darcy parameter D^{-1} . Lower the permeability of the porous medium lesser the fluid speed in the entire fluid region (Fig. 2). An increase in radiation-conduction number, K_1 has an adverse effect on the velocity due to steady mean flow (u_0) for all values of y . K_1 represents the relative contribution of thermal radiation heat transfer to thermal conduction heat transfer. For $K_1 < 1$ thermal conduction exceeds thermal radiation and for $K_1 > 1$ this situation is reversed. For $K_1 = 1$ the contribution from both modes is equal. In all cases steady mean flow velocity is a maximum at the plate ($y = 0$) and decays smoothly to the lowest value far from the plate (Fig. 3). Conversely an increase in free convection parameter, Grashof number Gr , boosts the steady mean flow velocity, (u_0). Increasing thermal buoyancy (Fig. 4) therefore accelerates the mean steady flow in particular at and near the plate surface. Fig.5 exhibits the magnitude of the velocity (u_0) increases with increase in the hall parameter m . Figures (6 to 17) correspond to the unsteady mean flow distributions due to the main flow (u_1) and also cross flow (w_1). The frequency of oscillation is prescribed as 2 unless otherwise indicated. Magnetic field effects on the unsteady mean main flow velocity component (u_1) and the unsteady mean cross flow velocity component (w_1), respectively, are presented in figures 6 and 12. The magnitude of the velocity (u_1) is strongly reduced with increase in the intensity of the magnetic field parameter M , with the maximum effect sustained at the plate surface where peak (u_1) value plummets from 0.037 for $M = 5$ to 0.0035 for $M = 10$ (Fig. 6). Unsteady mean cross flow velocity component (w_1) is also reduced in magnitude with a rise in M . For $M = 10$ cross flow velocity is almost totally suppressed at all locations transverse to the wall. With weaker magnetic field the backflow presence is substantial. As such very strong magnetic field may be applied in operations to successfully inhibit backflow normal to the plate surface (Fig. 12). The magnitude of the velocities (u_1 & w_1) reduces with increase in the inverse Darcy parameter D^{-1} . Lower the permeability of the porous medium the fluid speed retards in the entire fluid region (Fig. 7 & 13). Increasing radiation-conduction number, K_1 as with the steady mean flow (u_0) discussed in figure 3, again has an opposing influence on unsteady main flow velocity (u_1). The profiles are similar to those for steady mean flow. Conversely cross flow velocity (w_1) is positively affected by an increase in K_1 as depicted in figure (5). Profiles become less negative as K_1 rises from 1 through 2 to 3. As such backflow is inhibited considerably with increasing

thermal radiation. We observe that an unsteady mean cross flow velocity trough occurs near the plate surface at $y \sim 1$. At the plate cross flow velocity vanishes and at large distance from the plate again vanishes (Fig. 8 & 14). Figures 9 and 15 show the effect of Grashof number on the unsteady mean main flow velocity component (u_1) and the unsteady mean cross flow velocity component (w_1), respectively. In both cases increasing buoyancy has an adverse effect on both velocity fields. Mean flow velocity remains however positive always i.e., there is no presence of backflow. Cross flow velocity is consistently negative throughout the regime indicating that backflow is always present. Lower buoyancy forces i.e. smaller Grashof number serves to reduce the backflow. Very little effect of oscillation frequency (ω) is computed, in figure 10, on the unsteady mean main flow velocity component, (u_1) which decreases very slightly as ω rises from 2 through 4 to 6. However frequency exerts a marked influence on the unsteady mean cross flow velocity component (w_1), as shown in figure 16 which is decreased substantially with a rise in ω . Backflow is therefore augmented with increasing oscillation frequency, with the maximum effect at close proximity to the plate. In engineering design applications, therefore this region ($y \sim 1$) would be of particular interest in controlling backflow during MHD generator operations. The magnitudes of the velocities (u_1 and w_1) increase with increase in the hall parameter m (Fig. 11 & 17). The magnitude of the temperature θ_0 reduces with increase in radiation-conduction number K_1 due to steady mean flow (Fig. 18). The magnitude of the temperature θ_1 reduces with increase in K_1 and Pr due to unsteady mean flow (Fig. 19 & 20). Similarly the magnitude of the temperature θ_1 reduces with increase in K_1 and enhances with increase in Pr due to unsteady cross flow (Fig. 21 & 22). The magnitude of the temperature θ_1 reduces in $0 \leq y \leq 2.5$ and $y=4.5$ and enhances within the domain $2.5 < y < 4.5$ with increase in surface temperature oscillation ω due to unsteady mean flow (Fig. 23). Likewise the magnitude of the temperature θ_1 enhances in $0.5 \leq y \leq 1.5$ and reduces within the domain $2.5 \leq y \leq 4.5$ with increase in surface temperature oscillation ω due to unsteady cross flow (Fig. 24).

Tables (1-3) also show the combined influence of several of the dimensionless parameters on the shear stress at the plate. An increase in M and inverse Darcy parameter D^{-1} causes increase in the shear stress at the plate $y=0$ due to a steady mean flow (u_0) i.e. ω values become increasingly negative. Increasing radiation-conduction parameter, K_1 , hall parameter m and Grashof number Gr also decreases the shear stress i.e. decelerates the flow, in

consistency with the velocity distribution shown in figure (1-5) (Table. 1). Table (2) indicates that shear stress at the plate with unsteady mean flow due to main flow (u_1) reduces with increase in Gr , ω and m , and is greatly increased with an increase in the square root of the Hartmann magneto hydro dynamic number (M), inverse Darcy parameter D^{-1} and radiation-conduction parameter, K_1 . Unsteady mean flow is therefore enhanced strongly with an increase in magnetic field strength. An increase in thermal radiation-conduction number (K_1) also decreases values but very slightly indicating that thermal radiation has a very weak effect on flow at the plate surface. On the other hand, the shear stress at the plate with unsteady mean flow due to cross flow direction (w_1) as shown in table (3) is considerably increased with square root of the Hartmann magneto hydro dynamic number (M) since the magnetic retarding force acts in the same direction as this flow component and boosts secondary (cross) flow. A rise in thermal radiation-conduction number (K_1) also increases the slightly since values become less negative indicating that backflow is resisted with greater thermal radiation contribution. The shear stress enhances due to cross flow with increasing M , D^{-1} and ω , and reduces with increasing m , K_1 and Gr . An increase in frequency of oscillation (ω) causes the temperature gradient at the plate due to unsteady mean flow i.e. to decrease slightly, as indicated in table 4; conversely increasing thermal radiation-conduction parameter (K_1) has a strong positive effect inducing a major increase in Temperature gradient at the plate due to unsteady cross flow affected more strongly (Table. 5) with an increase in frequency of oscillation (ω), being reduced from -0.03531 for $\omega = 2$, to -0.07036 for $\omega = 4$ and to the lowest value of -0.10491 for $\omega = 6$ (all at $K_1 = 1$). In contrast to this the temperature gradient, is increased somewhat with an increase in thermal radiation-conduction parameter (K_1), for any value of ω . The combined influence of thermal radiation-conduction parameter (K_1) and Prandtl number (Pr) on the temperature gradient at the plate due to unsteady main flow is shown in (table. 6). An increase in thermal radiation-conduction parameter (K_1) substantially decreases values for all Prandtl numbers. An increase in Prandtl number also decreases values. Lower Pr values imply a higher thermal conductivity and correspond to liquid metals ($Pr \ll 1$). $Pr = 1$ implies that energy and momentum are diffused at the same rate and the lowest value of occurs for $Pr = 1$, at a given value of K_1 . Finally in table 7, temperature gradient at the plate due to unsteady cross flow, is observed to be increased with an elevation in thermal radiation-conduction parameter (K_1) at any Prandtl number (Pr). Conversely increasing Prandtl number markedly reduces the value of at a fixed value of K_1 . A similar trend was observed in the

earlier studies of for example Duwairi and Damsch [8], Raptis *et al.* [18] and more recently by Samad *et al.* [19]. The analytical solutions presented therefore provide a succinct confirmation of earlier results and also reveal some new interesting phenomena in the interaction of radiation, magnetic field and effect of hall current, porous medium and periodicity of surface temperature.

IV. FIGURES AND TABLES

3.1. Velocity Distributions due to steady mean flow

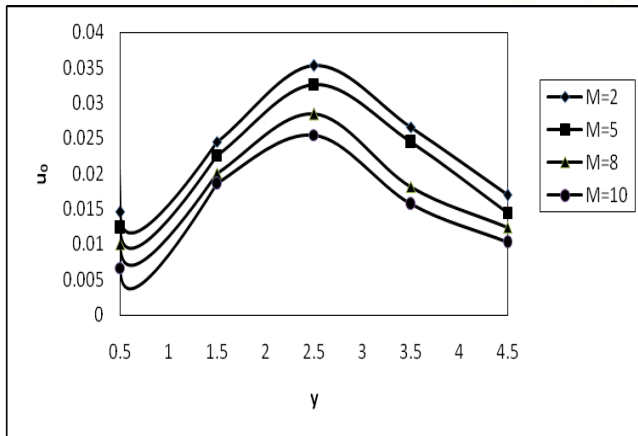


Fig. 1: Velocity distribution due to a steady mean flow for various M with $\omega = 0$, $Gr=2$, $D^{-1}=1000$, $m=1$, $K_1=1$, $Pr=0.025$

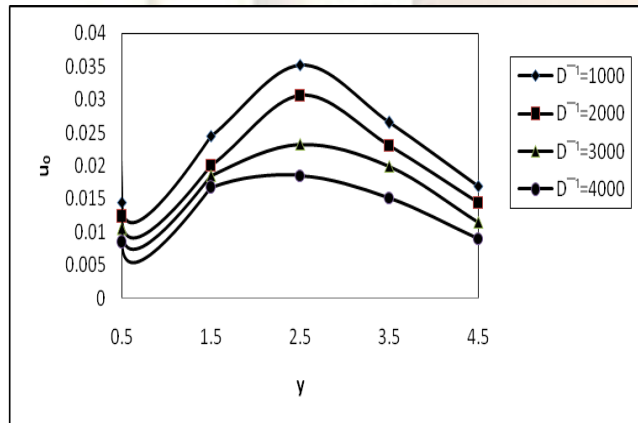


Fig. 2: Velocity distribution due to a steady mean flow for various D^{-1} with $\omega = 0$, $Gr=2$, $m=1$, $M=2$, $K_1=1$, $Pr=0.025$

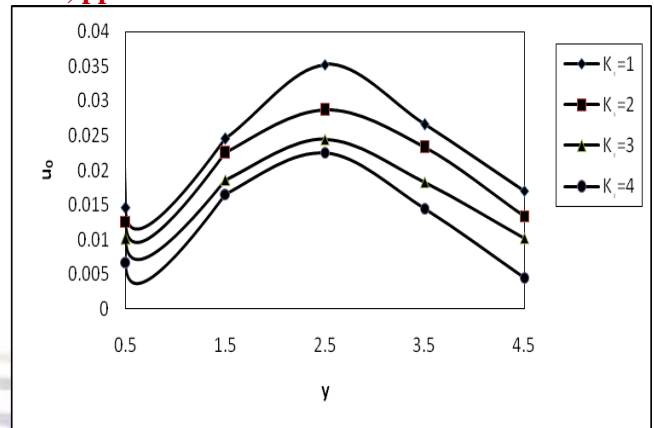


Fig. 3: Velocity distribution due to a steady mean flow for various K_1 with $\omega = 0$, $Gr=2$, $m=1$, $M=2$, $D^{-1}=1000$, $Pr=0.025$

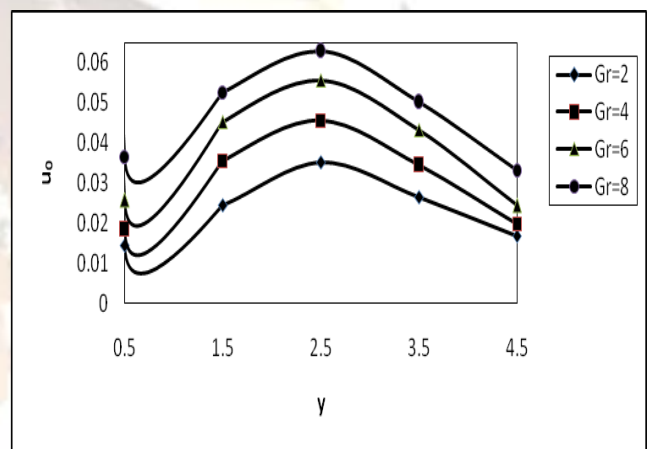


Fig. 4: Velocity distribution due to a steady mean flow for various Gr with $\omega = 0$, $M=2$, $m=1$, $D^{-1}=1000$, $K_1=1$, $Pr=0.025$

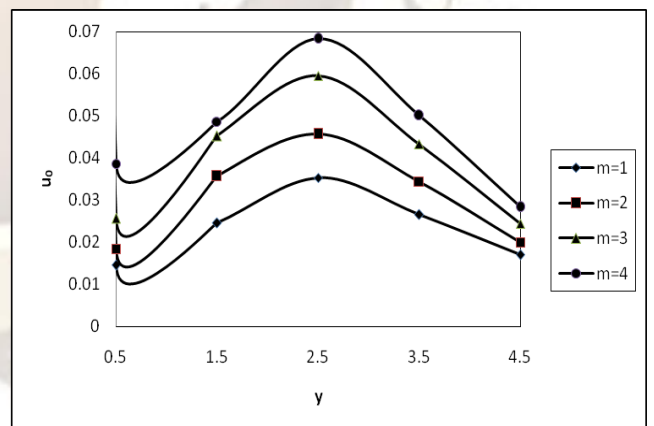


Fig. 5: Velocity distribution due to a steady mean flow for various m with $\omega = 0$, $M=2$, $Gr=12$, $D^{-1}=1000$, $K_1=1$, $Pr=0.025$

3.2. Velocity Distributions due to unsteady mean and cross flow

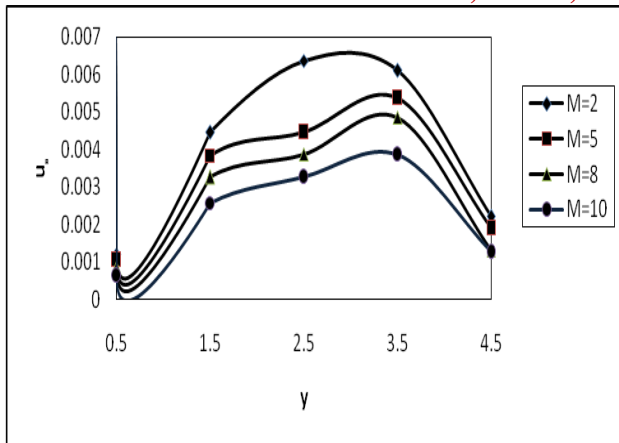


Fig. 6: Unsteady mean flow distribution due to mean flow for various M with $\omega = 2$, $Gr=2$, $m=1$, $D^{-1}=1000$, $K_1=1$, $Pr=0.025$

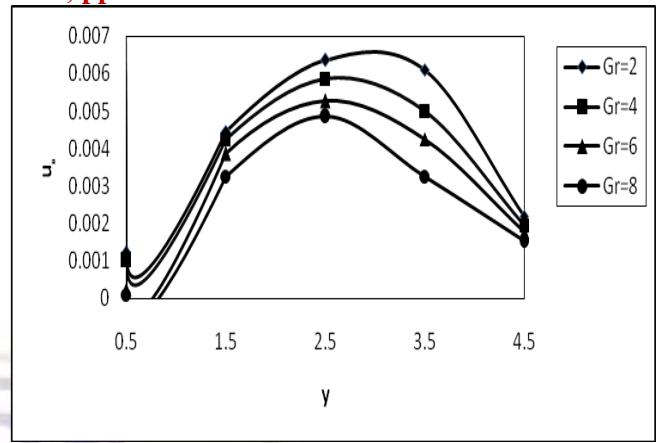


Fig. 9: Unsteady mean flow distribution due to mean flow for various Gr with $\omega = 2$, $M=2$, $D^{-1}=1000$, $m=1$, $K_1=1$, $Pr=0.025$

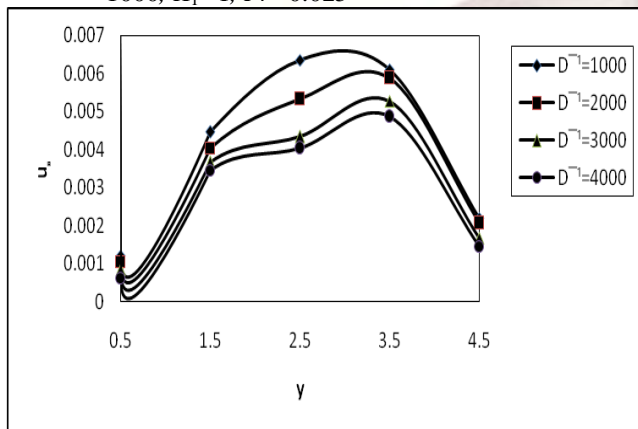


Fig. 7: Unsteady mean flow distribution due to mean flow for various D^{-1} with $\omega = 2$, $Gr=2$, $M=2$, $m=1$, $K_1=1$, $Pr=0.025$

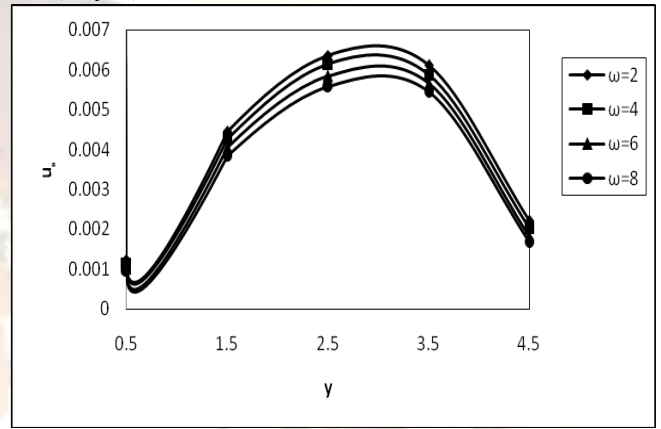


Fig. 10: Unsteady mean flow distribution due to mean flow for various ω with $Gr = 2$, $M=2$, $m=1$, $D^{-1}=1000$, $K_1=1$, $Pr=0.025$

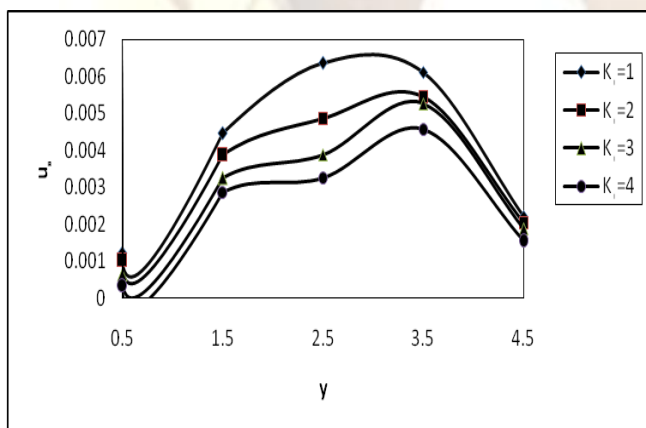


Fig. 8: Unsteady mean flow distribution due to mean flow for various K_1 with $\omega = 2$, $Gr=2$, $m=1$, $D^{-1}=1000$, $M=2$, $Pr=0.025$

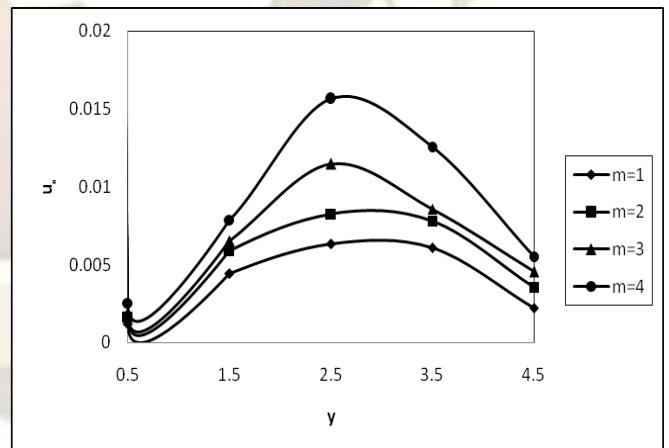


Fig. 11: Unsteady mean flow distribution due to cross flow for various m with $Gr = 2$, $M=2$, $\omega = 2$, $D^{-1}=1000$, $K_1=1$, $Pr=0.025$

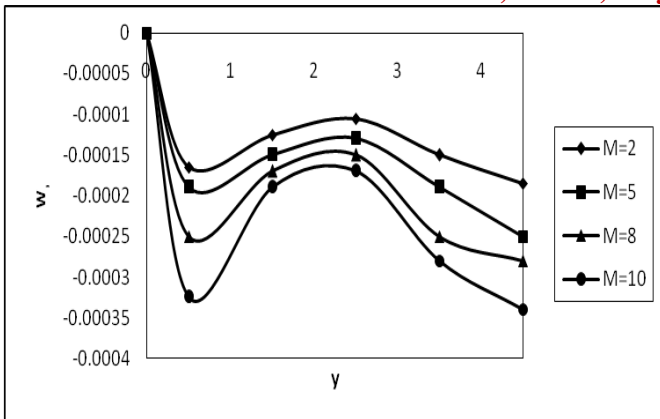


Fig. 12: Unsteady mean flow distribution due to cross flow for various M with $\omega = 2$, $Gr=2$, $m=1$, $D^{-1}=1000$, $K_1=1$, $Pr=0.025$

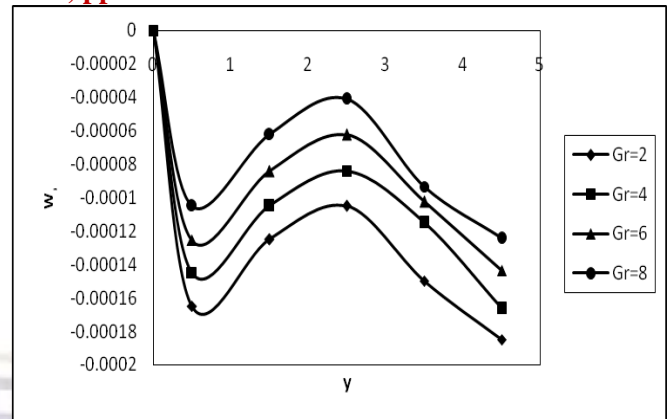


Fig. 15: Unsteady mean flow distribution due to cross flow for various Gr with $\omega = 2$, $M=2$, $m=1$, $D^{-1}=1000$, $K_1=1$, $Pr=0.025$

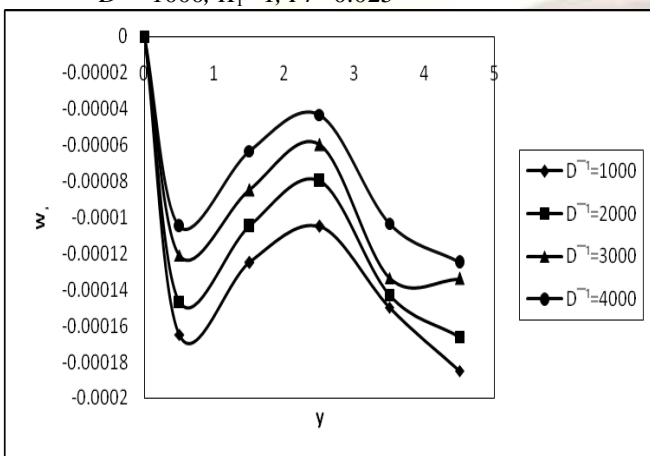


Fig. 13: Unsteady mean flow distribution due to cross flow for various D^{-1} with $\omega = 2$, $Gr=2$, $m=1$, $M=2$, $K_1=1$, $Pr=0.025$

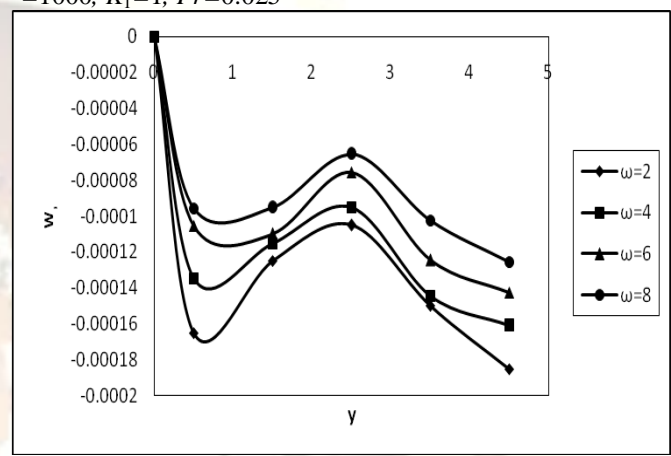


Fig. 16: Unsteady mean flow distribution due to cross flow for various ω with $Gr=2$, $M=2$, $m=1$, $D^{-1}=1000$, $K_1=1$, $Pr=0.025$

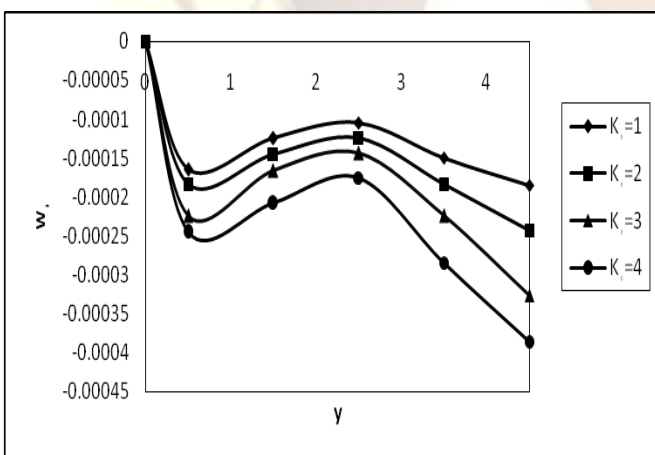


Fig. 14: Unsteady mean flow distribution due to cross flow for various K_1 with $\omega = 2$, $Gr=2$, $m=1$, $D^{-1}=1000$, $M=2$, $Pr=0.025$

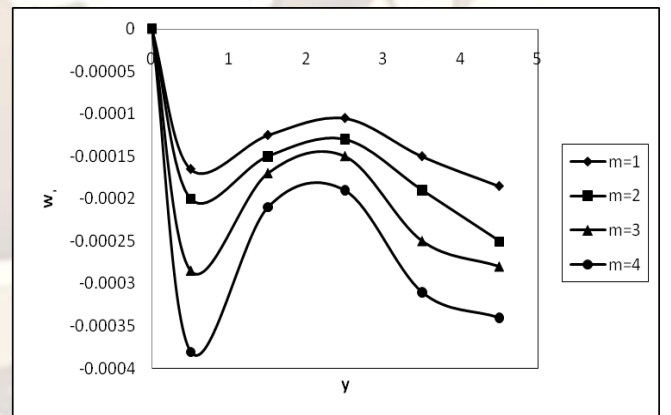


Fig. 17: Unsteady mean flow distribution due to cross flow for various m with $Gr=2$, $M=2$, $\omega=2$, $D^{-1}=1000$, $K_1=1$, $Pr=0.025$

3.3. Temperature Distributions due to steady flow

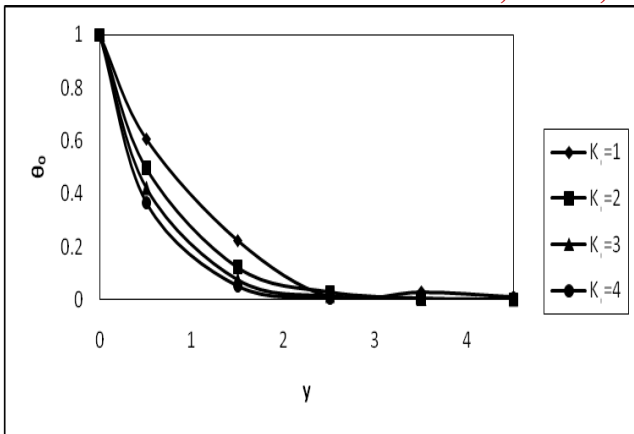


Fig. 18: Temperature distribution due to a steady mean flow for various K_1 with $\omega=0$

3.4. Temperature Distributions due to unsteady mean and cross flow

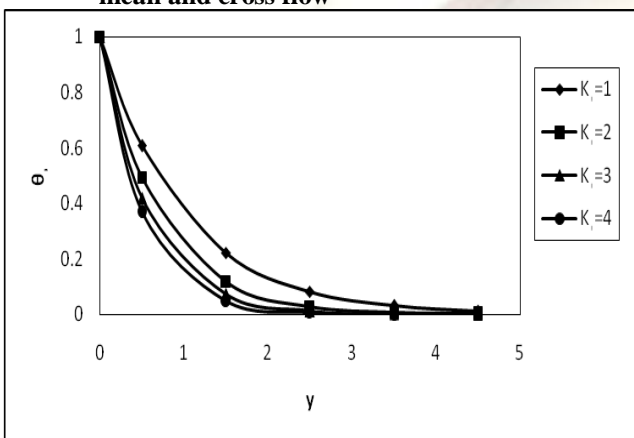


Fig. 19: Temperature distribution due to a unsteady mean flow for various K_1 with $\omega=2$, $Pr=0.025$

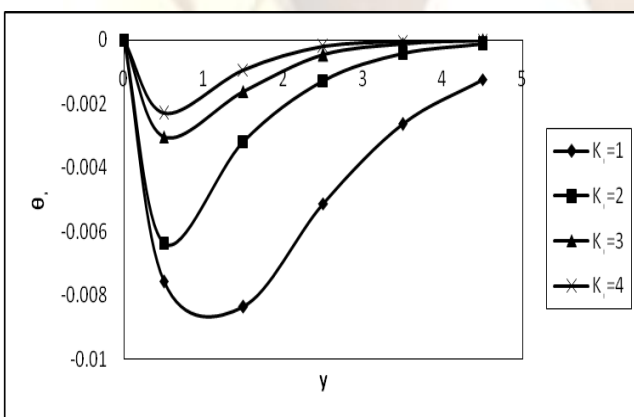


Fig. 20: Temperature distribution due to a unsteady mean flow for various K_1 with $\omega=2$, $Pr=0.025$

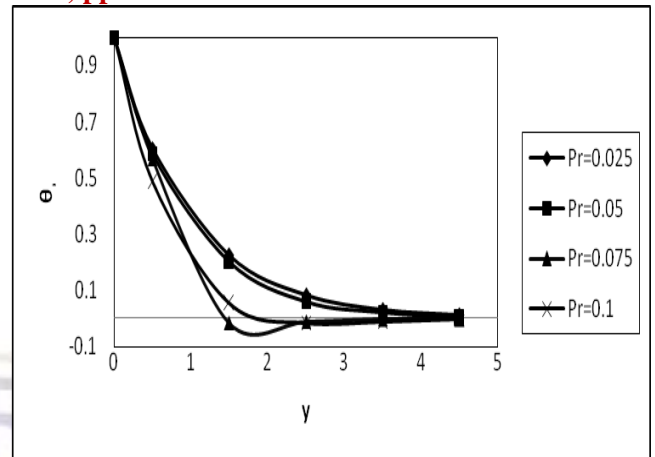


Fig. 21: Temperature distribution due to a unsteady mean flow for various Pr with $\omega=2$, $K_1=1$

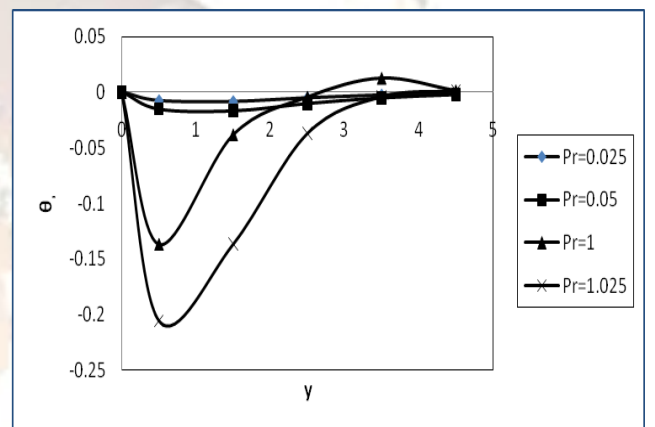


Fig. 22: Temperature distribution due to a unsteady mean flow for various Pr with $\omega=2$, $K_1=1$

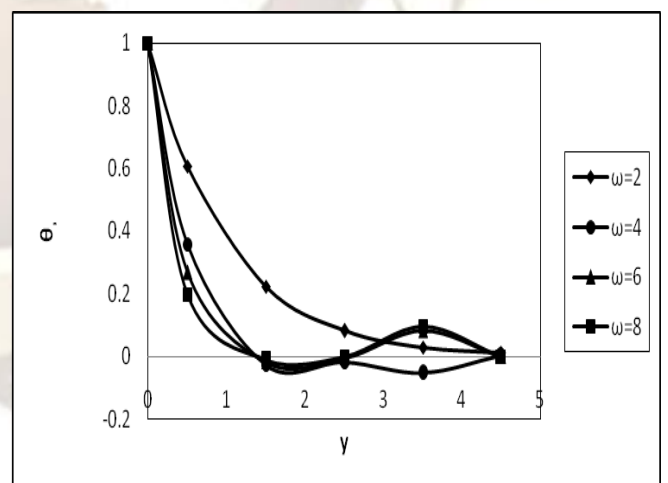


Fig. 23: Temperature distribution due to a unsteady mean flow for various ω with $Pr=0.025$, $K_1=1$

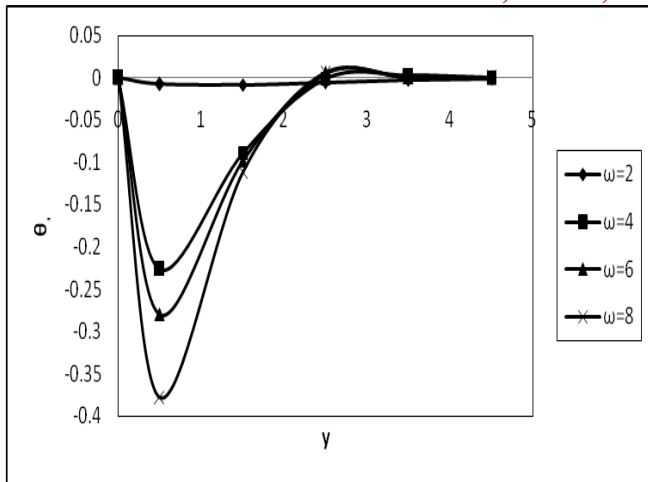


Fig. 24: Temperature distribution due to a unsteady mean flow for various ω with $Pr=0.025$, $K_1=1$

V. CONCLUSIONS

Exact solutions have been derived using complex variables for the transient Magneto hydro dynamic convection flow of an electrically-conducting, Newtonian, optically-thin fluid from a flat plate with thermal radiation and surface temperature oscillation effects. Our analysis has shown that:

1. Steady mean flow velocity, (u_0), is decreased with increasing thermal radiation (K_1), inverse Darcy parameter D^{-1} and magnetic hydro dynamic parameter (M), increased with Grashof number (Gr) and hall parameter m .
2. Unsteady mean flow velocity (u_1) is reduced with increasing radiation-conduction number, K_1 , slightly decreases with increasing frequency of oscillation (ω) and also falls with a rise in Grashof number, inverse Darcy parameter D^{-1} and magnetic hydro dynamic parameter, M . Mean flow velocity (u_1) is enhanced with increasing hall parameter m .
3. Conversely cross flow velocity (w_1) is increased with a rise in K_1 but decreased with a rise in Gr , D^{-1} and ω . Strong magnetic field also practically eliminates backflow.
4. The magnitude of the temperature θ_0 reduces with increase in radiation-conduction number K_1 due to steady mean flow.

5. The magnitude of the temperature θ_1 reduces with increase in K_1 and Pr due to unsteady mean flow. The magnitude of the temperature θ_1 reduces with increase in K_1 and enhances with increase in Pr due to unsteady cross flow.
6. The magnitude of the temperature θ_1 reduces in $0 \leq y \leq 2.5$ and $y=4.5$ and enhances within the domain $2.5 < y < 4.5$ with increase in surface temperature oscillation ω due to unsteady mean flow. Likewise the magnitude of the temperature θ_1 enhances in $0.5 \leq y \leq 1.5$ and reduces within the domain $2.5 \leq y \leq 4.5$ with increase in surface temperature oscillation ω due to unsteady cross flow.
7. An increase in M and inverse Darcy parameter D^{-1} causes increase in the shear stress at the plate $y=0$ due to a steady mean flow (u_0). Increasing radiation-conduction parameter, K_1 , hall parameter m and Grashof number Gr also decreases the shear stress.
8. The shear stress at the plate with unsteady mean flow due to main flow (u_1) reduces with increase in Gr , m and ω , and is greatly increased with an increase in the square root of the Hartmann magneto hydro dynamic number (M), inverse Darcy parameter D^{-1} and radiation-conduction parameter, K_1 .
9. The shear stress enhances due to cross flow with increasing M , D^{-1} and ω , and reduces with increasing K_1 , m and Gr .
10. Temperature gradient at the plate due to unsteady cross flow is reduced substantially with an increase in frequency of oscillation but elevated with an increase in thermal radiation-conduction parameter (K_1), for any value of ω .
11. An increase in thermal radiation-conduction parameter (K_1) reduces strongly as does an increase in Prandtl number (Pr).
12. Temperature gradient at the plate due to unsteady cross flow, increases with thermal radiation-conduction parameter (K_1) but reduces with a rise in Prandtl number.

Table 1: Shear stress (τ) at the plate $y=0$ due to a steady mean flow (u_0) for various values of thermal radiation-conduction number (K_1), square root of the Hartmann magneto hydro dynamic number (M), Gr and m or $\omega = 0$

M	I	II	III	IV	V	VI	VII	VIII	IX
2	-2.45655	-2.84415	-2.99445	-2.74445	-2.85856	-1.52498	-1.11489	-2.15526	-2.00145
5	-4.64789	-4.83145	-5.26688	-4.73365	-4.75698	-2.44565	-2.00534	-4.15585	-3.88859
8	-6.25566	-6.33475	-6.33248	-6.25446	-6.53266	-4.45244	-3.21156	-5.62281	-4.66525
10	-9.66655	-9.81498	-10.1156	-9.75278	-9.84422	-6.22415	-5.00012	-7.99859	-5.23011

	I	II	III	IV	V	VI	VII	VIII	IX
D^{-1}	1000	2000	3000	1000	1000	1000	1000	1000	1000
K_1	1	1	1	2	3	1	1	2	1

<i>Gr</i>	2	2	2	2	2	2	4	6	2	2
<i>m</i>	1	1	1	1	1	1	1	1	2	3

Table 2: Shear stress (τ) at the plate $y=0$ with unsteady mean flow due to main flow (u_1) for various values of frequency of oscillation (ω) and square root of the Hartmann magneto hydro dynamic number (M), K_1 , Gr , m and $Pr = 0.025$

<i>M</i>	I	II	III	IV	V	VI	VII	VIII	IX	X	XI
2	-22.714	-31.971	-39.088	-22.714	-22.714	-22.665	-23.284	-22.714	-22.714	-22.612	-22.452
5	-22.946	-32.141	-39.218	-22.945	-22.947	-22.904	-22.626	-22.945	-22.945	-22.854	-22.665
8	-23.374	-32.442	-39.464	-23.374	-23.375	-23.331	-22.861	-23.374	-23.372	-23.356	-23.152
10	-23.762	-32.722	-39.694	-23.762	-23.762	-23.718	-23.676	-23.762	-23.764	-23.511	-23.354

	I	II	III	IV	V	VI	VII	VIII	IX	X	XI
D^{-1}	1000	2000	3000	1000	1000	1000	1000	1000	1000	1000	1000
K_1	1	1	1	2	3	1	1	1	1	1	1
<i>Gr</i>	2	2	2	2	2	4	6	2	2	2	2
ω	2	2	2	2	2	2	2	4	6	2	2
<i>m</i>	1	1	1	1	1	1	1	1	1	2	3

Table 3: Shear stress (τ) at the plate $y=0$ with unsteady mean flow due to cross flow (u_1) for various values of frequency of oscillation (ω), square root of the Hartmann magneto hydro dynamic number (M), K_1 , Gr , m and $Pr = 0.025$

<i>M</i>	I	II	III	IV	V	VI	VII	VIII	IX	X	XI
2	-22.008	-31.268	-38.377	-22.005	-22.004	-21.945	-21.045	-22.004	-22.004	-15.486	-13.895
5	-22.234	-31.435	-38.511	-22.238	-22.238	-22.125	-21.945	-22.215	-22.245	-18.225	-15.445
8	-22.665	-31.734	-38.764	-22.666	-22.665	-22.625	-22.169	-22.666	-22.665	-20.562	-18.452
10	-23.0585	-31.017	-38.988	-23.053	-23.053	-23.049	-22.982	-23.052	-23.054	-21.468	-19.256

	I	II	III	IV	V	VI	VII	VIII	IX	X	XI
D^{-1}	1000	2000	3000	1000	1000	1000	1000	1000	1000	1000	1000
K_1	1	1	1	2	3	1	1	1	1	1	1
<i>Gr</i>	2	2	2	2	2	4	6	2	2	2	2
ω	2	2	2	2	2	2	2	4	6	2	2
<i>m</i>	1	1	1	1	1	1	1	1	1	2	3

Table 4: Temperature gradient at the plate due to unsteady main flow for various values of frequency of oscillation (ω) and thermal radiation-conduction parameter (K_1) for $Pr = 0.025$.

ω	I	II	III
2	-1.00000	-1.41432	-1.73214
4	-1.00125	-1.41466	-1.73228
6	-1.00279	-1.41521	-1.73246
8	-1.00424	-1.41732	-1.73284
K_1	1	2	3

Table 5: Temperature gradient at the plate due to unsteady cross flow for various values of frequency of oscillation (ω) and thermal radiation-conduction parameter (K_1) with $Pr = 0.025$

ω	I	II	III
2	-0.02499	-0.01768	-0.01532
4	-0.04993	-0.03534	-0.02894
6	-0.07479	-0.05299	-0.03566
8	-0.09222	-0.06735	-0.04225
K_1	1	2	3

Table 6: Temperature gradient at the plate due to unsteady main flow for various values of thermal radiation-conduction parameter (K_1) and Prandtl number (Pr) with $\omega = 2$

K_1	I	II	III	IV	V
1	-1.28082	-1.00125	-1.00045	-1.32049	-1.46635
2	-1.55949	-1.41462	-1.32645	-1.84538	-1.94522
3	-1.82125	-1.73229	-1.63322	-2.00536	-2.14455
4	-2.06095	-2.00019	-1.98882	-2.11432	-2.16654
	I	II	III	IV	V
Pr	0.025	0.05	0.075	0.025	0.025
ω	2	2	2	4	6

Table 7: Temperature gradient at the plate due to unsteady cross flow for various values of thermal radiation-conduction parameter (K_1) and Prandtl number (Pr) with $\omega=2$

K_1	I	II	III	IV	V
1	-0.80022	-0.04992	-0.02452	-0.95263	-1.14362
2	-0.65725	-0.03534	-0.02965	-0.83452	-0.93163
3	-0.56289	-0.02885	-0.00145	-0.67425	-0.84435
4	-0.49734	-0.02496	-0.00035	-0.05921	-0.62432
	I	II	III	IV	V
Pr	0.025	0.05	0.075	0.025	0.025
ω	2	2	2	4	6

ACKNOWLEDGEMENTS

We kindly acknowledge Late Prof. D.V.Krishna, Department of Mathematics, Sri Krishnadevaraya University, Anantapur (Andhra Pradesh), India for their useful remarks on the manuscript and Prof. R. Siva Prasad, Department of Mathematics, Sri Krishnadevaraya University, Anantapur (AP), India for providing the material which was used to validate our computational work. Also, part of the computational facilities was provided by Department of Mathematics, Rayalaseema University, Kurnool (AP), India.

REFERENCES

- [1]. Aboeldahab E.M. and El-Din. A.A.G. (2005): "Thermal radiation effects on MHD flow past a semi-infinite inclined plate in the presence of mass diffusion", *Heat & Mass Transfer*, 41(12), pp. 1056-1065.
- [2]. Alagoa. K.D., Tay. G. and Abbey. T.M. (1998): "Radiative and free convective effects of MHD flow through a porous medium between infinite parallel plates with time-dependent suction". *Astrophysics and Space Science*, 260(4), pp. 455-468.
- [3]. Alam. M.S., M.M. Rahman, and M.A. Sattar (2008): "Effects of variable suction and thermophoresis on steady MHD combined free-forced convective heat and mass transfer flow over a semi-infinite permeable inclined plate in the presence of thermal radiation". *Int. J. Thermal Sciences*, 47(6), pp. 758-765.
- [4]. Anwerbeg. O and S.K. Ghosh (2010): "Analytical study of magneto hydro dynamic radiation-convection with surface temperature oscillation and secondary flow effects", *Int. J. of Appl. Math and Mech.* 6 (6), pp. 1-22.
- [5]. Audunson.T. and Gebhart.B. (1972): "An experimental and analytical study of natural convection with appreciable thermal radiation effects", *J. Fluid Mechanics*, 52(1), pp. 57-95.
- [6]. Bestman. A.R. (1989): "Radiative transfer to oscillatory hydro magnetic rotating flow of a rarefied gas past a horizontal flat plate". *Int. J. Numerical Methods in Fluids*, 9(4), pp. 375-384.
- [7]. Duwairi.H.M. (2005): "Viscous and Joule heating effects on forced convection flow from radiate isothermal porous surfaces", *Int. J. Numerical Methods Heat Fluid Flow*, 15(5), pp. 429-440.
- [8]. Duwairi.H.M. and Damseh.R.A), pp. 57-95.
- [9]. Bestman. A.R. (1989): "Radiative transfer to oscillatory hydro magnetic rotating flow of a rarefied gas past a horizontal flat plate". *Int. J. Numerical Methods in Fluids*, 9(4), pp. 375-384.
- [10]. Duwairi.H.M. (2005): "Viscous and Joule heating effects on forced convection flow from radiate isothermal porous surfaces. (2004): "Magneto hydro dynamic natural convection heat transfer from radiate vertical porous surfaces", *Heat Mass Transfer*, 40(10), pp. 787-792.
- [11]. Duwairi.H.M. and Duwairi.R.M. (2005): "Thermal radiation effects on MHD-Rayleigh flow with constant surface heat flux", *Heat and Mass Transfer*, 41(1), pp. 51-57.
- [12]. El-Hakiem.M.A. (2000): "MHD oscillatory flow on free convection radiation through a porous medium with

- constant suction velocity”, *J. Magnetism Magnetic Materials*, 220(2-3), pp. 271-276.
- [13]. Ghosh.S.K. and Pop.I. (2007): “Thermal radiation of an optically-thick gray gas in the presence of indirect natural convection”, *Int. J. Fluid Mechanics Research*, 34(6), pp. 515-520.
- [14]. Helliwell. J.B. and Mosa. M.F. (1979): “Radiative heat transfer in horizontal magneto hydro dynamic channel flow with buoyancy effects and an axial temperature gradient”, *Int. J. Heat Mass Transfer*, 22, pp. 657-668.
- [15]. Hughes. W.F. and Young. F.J. (1966): *The Electro magneto dynamics of Fluids*, John Wiley and Sons, New York, USA.
- [16]. Israel-Cookey.C, A. Ogulu, and V.B. Omubo-Pepple. (2003): “Influence of viscous dissipation and radiation on unsteady MHD free-convection flow past an infinite heated vertical plate in a porous medium with time-dependent suction”, *Int. J. Heat and Mass Transfer*, 46(13), pp. 2305-2311.
- [17]. Larson.D.W. and R.Viskanta. (1976): “Transient combined laminar free convection and radiation in a rectangular enclosure”, *J. Fluid Mechanics*, 78(1), pp. 65-85.
- [18]. Meyer. R.C. (1958): “On reducing aerodynamic heat-transfer rates by magneto hydro dynamic techniques”, *J. Aerospace Sciences*, 25, pp. 561- 566.
- [19]. Ouaf. M.E.M. (2005): “Exact solution of thermal radiation on MHD flow over a stretching porous sheet”, *Applied Mathematics and Computation*, 170(2), pp. 1117-1125.
- [20]. Raptis.A, Perdikis.C, and Takhar.H.S. (2004): “Effect of thermal radiation on MHD flow”. *Applied Mathematics and Computation*, 153(3), pp. 645-649.
- [21]. Samad. M.A. and Rahman. M.M. (2006): “Thermal radiation interaction with unsteady MHD flow past a vertical porous plate immersed in a porous medium”, *J. Naval Architecture and Marine Engineering*, 3, pp. 7-14.
- [22]. Shercliff. J.A. (1965): *A Textbook of Magneto hydro dynamics*, Cambridge University Press, UK.
- [23]. Siegel. R. and Howell. J.R. (1993): *Thermal Radiation Heat Transfer*, Hemisphere, USA.
- [24]. Vasil’ev. E.N. and D.A. Nesterov. (2005): “The effect of radiative-convective heat transfer on the formation of current layer”, *High Temperature*, 43(3), pp. 396-403.
- [25]. Yasar. O. and Moses. G.A. (1992): “R-MHD: an adaptive-grid radiation-magneto hydro dynamics computer code”. *Computer Physics Communications*, 69(2-3), pp. 439-458.
- [26]. Zueco. J. (2007): “Network simulation method applied to radiation and viscous dissipation effects on MHD unsteady free convection over vertical porous plate”, *Applied Mathematical Modelling*, 31(9), pp. 2019-2033.

Appendix:

$$\alpha = K_1 - \left(\frac{M^2}{1+m^2} + D^{-1} \right), \quad \beta = \omega(\text{Pr}-1),$$

$$C_1 = \frac{1}{\sqrt{2}} \left[\left(\frac{M^2}{1+m^2} + D^{-1} \right)^2 + \omega^2 \right]^{\frac{1}{2}} + \left(\frac{M^2}{1+m^2} + D^{-1} \right)^{\frac{1}{2}}$$

$$D_1 = \frac{1}{\sqrt{2}} \left[\left(\frac{M^2}{1+m^2} + D^{-1} \right)^2 + \omega^2 \right]^{\frac{1}{2}} - \left(\frac{M^2}{1+m^2} + D^{-1} \right)^{\frac{1}{2}}$$

$$C_2 = \frac{1}{\sqrt{2}} \left[\left(K_1^2 + \omega^2 P_r^2 \right)^{\frac{1}{2}} + K_1 \right]^{\frac{1}{2}},$$

$$D_2 = \frac{1}{\sqrt{2}} \left[\left(K_1^2 + \omega^2 P_r^2 \right)^{\frac{1}{2}} - K_1 \right]^{\frac{1}{2}},$$